

---

# Delivery of a new ACS SBC throughput curve for Synphot

Francesca R. Boffi, M. Sirianni, R. A. Lucas, N. R. Walborn, C. R. Proffitt  
April 18, 2008

---

## ABSTRACT

*On November 12th, 2007 a new ACS SBC throughput curve was implemented in CDBS, OPUS and DADS. This new curve is an improved version and accounts for the SBC red leak. The red leak portion is based on a spectrum of HD 209458 prepared by Paul Goudfrooij.*

---

## Pre-November 2007

In late Spring 2007, analysis of SBC observations of flux calibration stars and a G-type star using the SBC PR110L prism revealed that the sensitivity of the MAMA detector to optical and near-IR light is apparently much larger than previously thought. Some preliminary work was done at ST-ECF and a revised total transmission curve for the SBC with the PR110L prism, shown in Figure 1, was provided. The SBC spectral response is defined by the cutoff of the MgF2 window at 1150 Å at short wavelengths, and by the relatively steep decline of the CsI photocathode at long wavelengths.

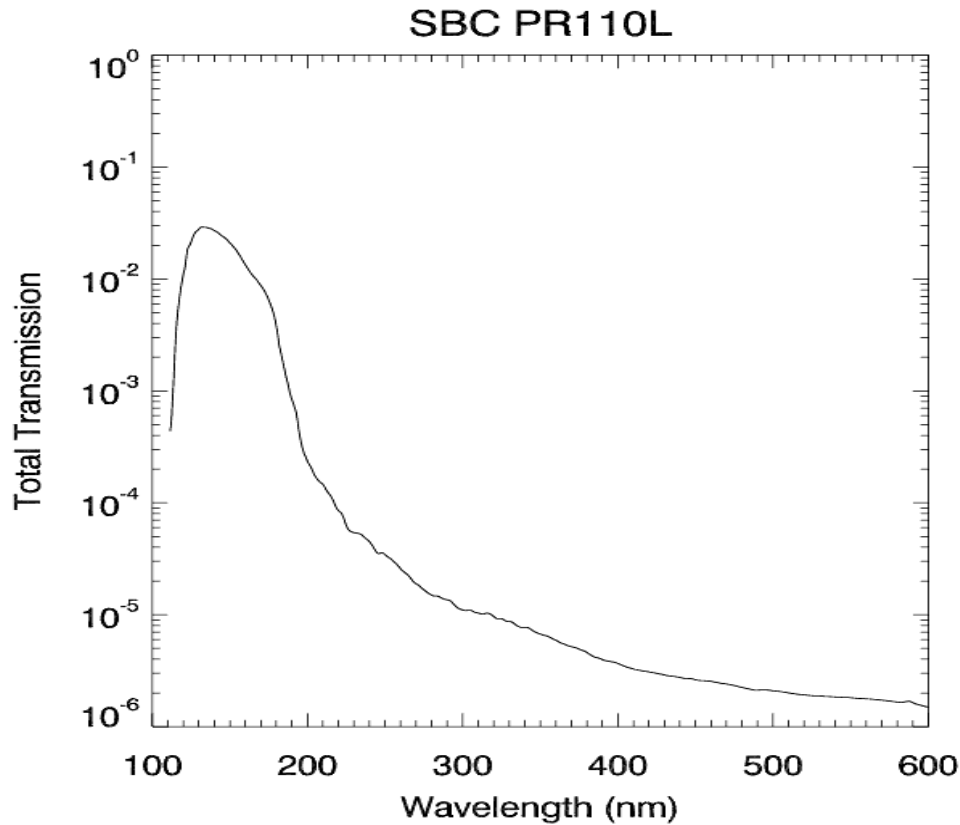


**Figure 1:** Total throughput of the SBC with the prism PR110L (from ST-ECF).

Preliminary estimates of the real SBC throughput indicate that the detector efficiency is factors of approximately 50 and 1000 higher at wavelengths of 3000 and 4000 Å respectively compared to ground testing. This may have a non-negligible impact on stellar observations since, for example, for a solar type spectrum, half of the detected photons are not the expected FUV photons. In addition, there is some evidence that this effect may possibly grow worse as the detector warms up, while it's not clear whether this effect has also been increasing during the lifetime of the SBC.

For observations taken through the prisms PR110L and PR130L, it is straightforward to identify the extra contribution from the red leak that clearly also affects SBC imaging observations done with the long pass filters. Until this effect is better understood and calibrated, extreme caution should be used when interpreting FUV imaging observations of red targets.

This information has been conveyed into the ACS Instrument Handbook (v. 8.0), where Figure 1 above corresponds to Fig. 4.17. In Table 1 we have quantified the visible light rejection for different stellar spectral energy distribution (Table 5.7 in the ACS Instrument Handbook) to help the users when planning their observations with the SBC.

**Table 1.**

Visible-light rejection of the SBC F115LP imaging mode. The stellar spectra are from the Pickles catalog (Pickles A.J., 1998, PASP 110, 863) and can be retrieved from the Synphot database (<ftp://ftp.stsci.edu/cdbs/cdbs2/grid/pickles>). The system throughput corresponds to the sensitivity plotted in Figure 1.

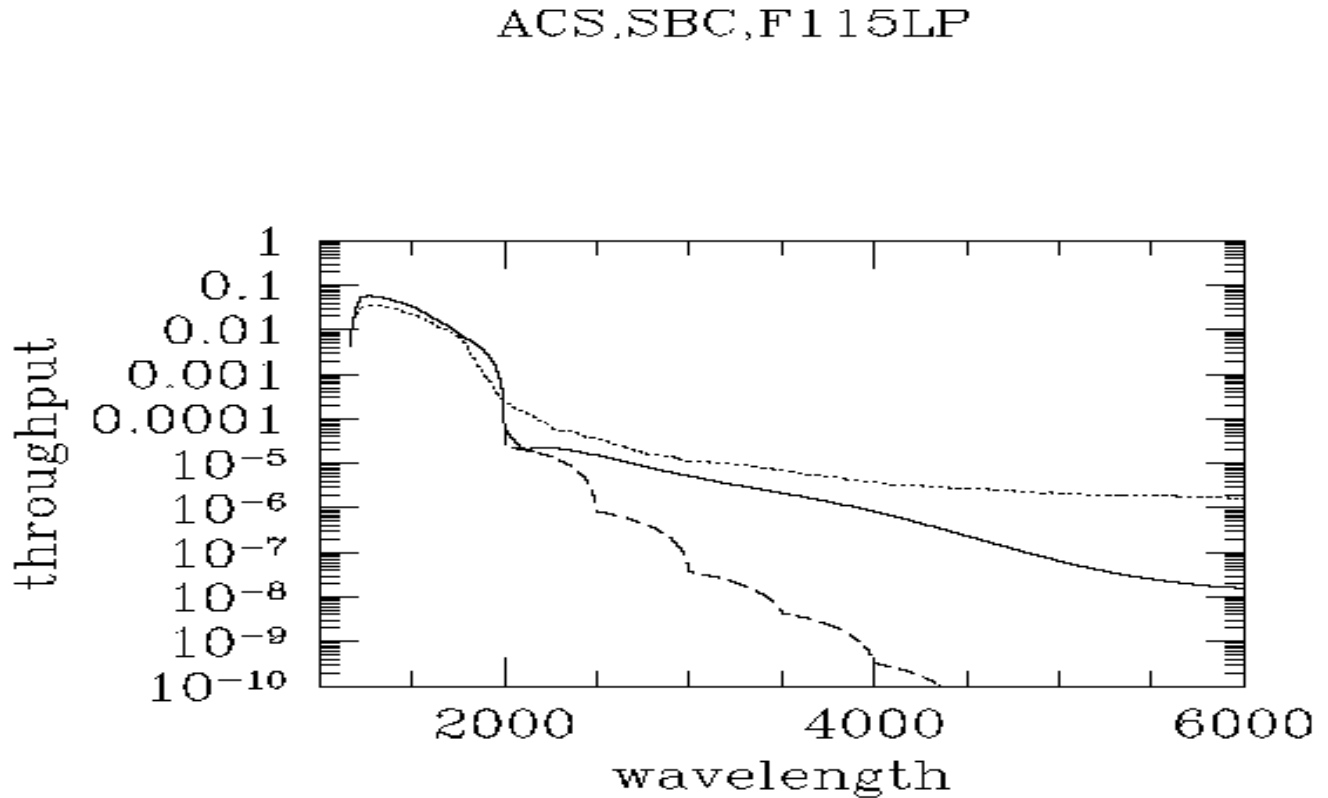
Stellar type	Percentage of all detected photons with $\lambda < 1800 \text{ \AA}$	Percentage of all detected photons with $\lambda < 3000 \text{ \AA}$
O5 V	97.7	100
B1 V	98.7	100
A0 V	95.6	99.7
G0 V	29.0	40.5
K0 V	0.	5.4

## November 2007 and beyond

While the work above was being performed, a second SBC throughput curve, with the red leak portion of a spectrum of the star HD 209458 with extensive STIS observations also available (prepared by Paul Goudfrooij) was provided to us. Figure 2 is a plot of three curves, each representing the total throughput for the “ACS,SBC,F115LP” observation mode, using the ST-ECF determination (dotted line), using the second sensitivity curve with the red leak portion as obtained from a spectrum of the standard star HD 209458 (solid line), and using the curve found in Synphot (dashed line; file `acs_sbc_mama_006_syn.fits`; ground version). The solid and dashed lines agree well in the FUV part of the spectrum, which is to be expected as the FUV part is in common for the two cases.

The red part of the curves are instead different and in particular the two newer curves account for the red leak differently.

**Figure 2:** Total throughput for the “ACS,SBC,F115LP” observation mode. See text for details on the three curves.



After Figure 2 was plotted, it was clear that further tests would need to be carried out to prove which of the two new sensitivities to trust (and deliver to the ETC/Synphot database). The first test that was performed was to estimate the count rate of a portion of Saturn’s spectrum. This test produced the correct answer when the solid line was adopted, while the dotted line produced a gross overestimate of the count rate.

A second test was to use a blue star (an O5 V star from Pickles’ atlas referenced above) and compare the plot obtained by convolving the stellar spectrum with the observation mode as available in Synphot (dashed curve), with the plot obtained convolving with the solid line. Again, as expected, both curves coincide, as the red part of the spectrum for a blue star should remain unaffected.

These tests, together with the fact that blue stars were used to measure the red leak for the dotted line, have led us to deliver to CDBS the SBC transmission curve as derived

from the solid line in Figure 2. The issue with deriving the red leak from blue standard stars is that with such stars it is impossible to separate scattering and the finite width of the LSF from the true red leak. In a spectrum that falls steeply towards the red, the count rate at any point will be dominated by photons that are really of rather shorter wavelength than the nominal ones at that position, because blue photons are more likely to scatter redward than red ones to scatter toward the blue. This problem is especially bad for prisms where the resolution is low.

Figure 3 represents the total SBC throughput as derived from Synphot using the reference file `acs_sbc_mama_syn_007.fits` for the sensitivity (the solid line in Fig.2). For this curve we recalculate the visible light rejection percentages as in Table 1 and we present them in Table 2. The most substantial differences are for the G0 V star type and can be explained because the newest SBC throughput lets in at 3000 Å a factor of 2.2 less photons than the ST-ECF throughput previously adopted.

**Figure 3:** The current total SBC throughput (observation mode “ACS,SBC”).

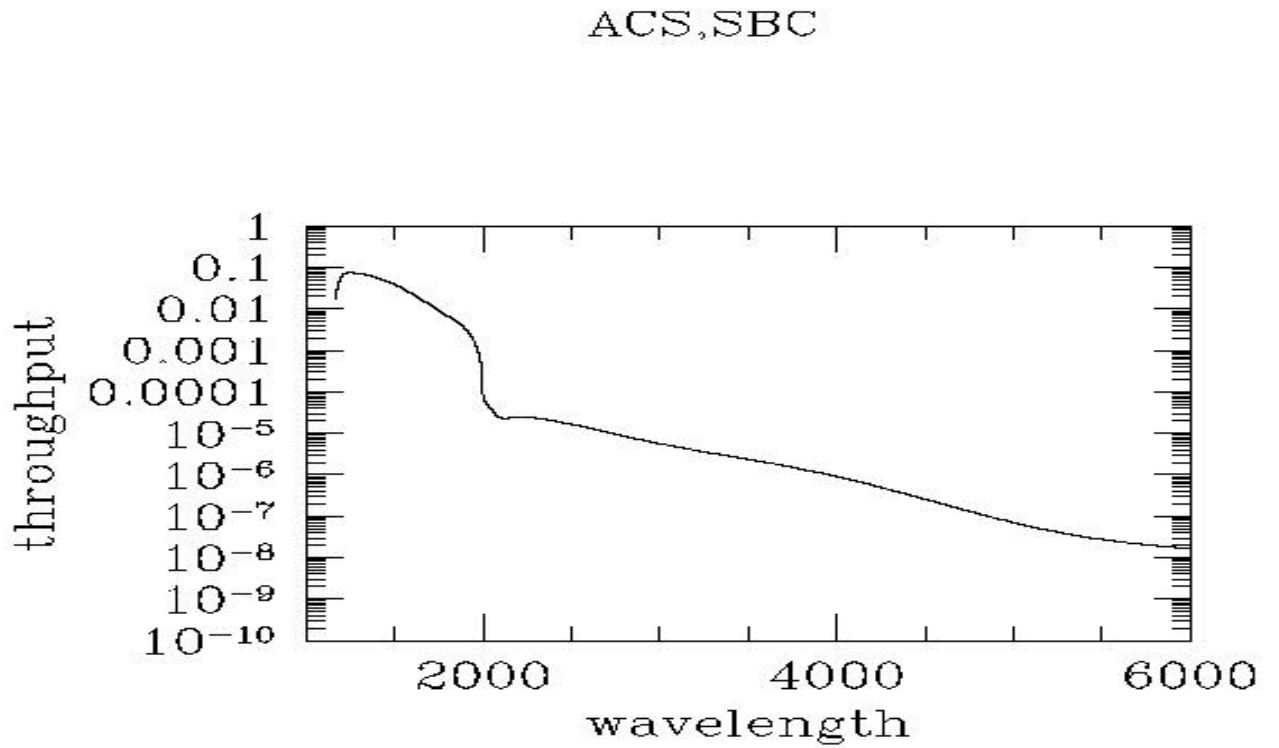


**Table 2.** Visible-light rejection of the SBC F115LP imaging mode when using the SBC throughput from Figure 3..

Stellar type	Percentage of all detected photons with $\lambda < 1800$ $\text{\AA}$	Percentage of all detected photons with $\lambda < 3000$ $\text{\AA}$
O5 V	96.7	100
B1 V	98.3	100
A0 V	94.1	100.
G0 V	72.0	86.0
K0 V	0.	16.8

### Bright Object protection limits

The revised sensitivity curve has been reflected in the ETC since November 2007. Hence, the V-magnitude screening limits in Table 7.4, Section 7.2.2 of the ACS Instrument Handbook are now fainter for stars later than type F0 V. Revised values are given in the following table.

All values have been calculated with the ETC to satisfy the local countrate screening limit of 50 counts/second/pixel (Table 7.3), and all other input sources are also as specified in the ACS Instrument Handbook, except that the KM III values are now the faintest for each spectral element among IUE data for eight objects with spectral types from G8 through M5. Note that many of the brightest pixel wavelengths for the prisms correspond to chromospheric emission lines.

**Table 3.** Revised bright-limit V-band magnitudes for observations with the SBC filters and prisms (no reddening).

Spec Type	F122M	F115LP	F125LP	F140LP	F150LP	F165LP	PR110L	PR130L
F0 V	4.8	10.1	10.0	10.0	10.0	9.9	8.3	8.3
F2 V	4.0	9.3	9.3	9.2	9.2	9.1	7.6	7.5
F5 V	2.2	7.7	7.6	7.6	7.6	7.5	5.9	5.9
F8 V	0.9	6.8	6.8	6.7	6.7	6.7	4.7	4.7
G2 V	2.2	6.3	6.0	6.0	5.9	5.8	3.2	3.1
G8 V	...	5.6	5.6	5.4	5.2	4.8	2.2	2.1
K2 V	...	5.7	5.7	5.2	5.0	4.3	3.2	3.0
KM III	...	4.5	4.5	4.2	4.0	3.6	2.7	2.3

(1) Values for objects of type F8 V and bluer are based on Kurucz models.

(2) G2 V values are based on the Solar template in the ACS ETC.

(3) G8 V values are based on IUE data for the star Tau Ceti.

(4) K2 V values are based on IUE data for the star Epsilon Eridani.

(5) KM III values are the faintest per spectral element from the IUE spectra of a set of 8 late-type stars.

**Table 4.** Brightest pixel wavelengths

Spec Type	PR110L	PR130L
F0 V	1792.17 Å	1799.96 Å
F2 V	1792.17 Å	1799.96 Å
F5 V	1886.44 Å	1890.16 Å
F8 V	1886.44 Å	1890.16 Å
G2 V	1886.44 Å	1890.16 Å
G8 V	1813.90 Å	1820.74 Å
K2 V	1548.18 Å	1550.03 Å
KM III	1304.07 Å	1302.78 Å

The individual stellar magnitude limits from IUE data used for the selection of the magnitude limits for KM III are shown below. Rather than an average value, the faintest value per each filter was chosen as the V magnitude limit for that filter. IUE spectra for use in devising KM III limits were not renormalized in the ETC, but the countrate results were scaled to find the appropriate V magnitude.

**Table 5.** IUE Stellar Spectra For Determining KM III Bright Object V-mag Limits.

Spec Class	Star ID	F115LP	F125LP	F140LP	F150LP	F165LP	PR110L	PR130L
G8 III	Mu Peg	4.5	4.5	4.2	4.0	3.6	1.3	1.4
K0 III	Eta Ser	4.5	4.4	4.2 *	4.0 *	3.6 *	0.9	0.9
K2 III	Alpha Boo	3.7	3.6	3.0	2.7	2.0	1.4	1.1
K3 II	Gamma Aql	4.0	4.0	3.5	3.1	2.2	2.7 *	2.3 *
M1 III	Delta Oph	3.3	3.3	2.7	2.4	1.2	1.9	1.5
M2 III	Alpha Cet	3.9	3.8	3.3	2.9	1.7	2.4	2.1
M5 III	V806 Cen	4.4	4.3	3.9	3.9	2.4	1.9	1.8
M5 III	Beta Gru	4.5 *	4.5 *	4.1	3.7	2.6	1.9	1.6

\* Denotes the adopted limits for a given spectral element. Note that Gamma Aql was used for both the KM III PR110L and PR130L values of "wavelength of brightest pixel" in Table 3.

## Summary

The SBC throughput curve delivered to Synphot on November 12th, 2007, and named `acs_sbc_mama_syn_007.fits`, was obtained using the red leak portion of the spectrum of HD 209458 by Paul Goudfrooij. This throughput is different from the one that was used in the ACS Instrument Handbook v. 8, and it will be incorporated there starting with v. 8.1. In this ISR we have outlined the red leak issue and described what we did to provide the most accurate SBC throughput available to the community. We have also provided the table with the corresponding bright object protection V magnitude limits.